Bistability of pulsating intensities for double-locked laser diodes

M. Nizette and T. Erneux
Université Libre de Bruxelles, Optique Nonlinéaire Théorique, Campus Plaine, Code Postal 231, 1050 Bruxelles, Belgium

A. Gavrielides and V. Kovanis
Nonlinear Optics Center, Air Force Research Laboratory, 3550 Aberdeen Avenue SE, Kirtland Air Force Base, New Mexico 87117-5776

T. B. Simpson
Jaycor, Inc., P. O. Box 85154, San Diego, California 92186-5154
(Received 17 August 2001; published 8 May 2002)

Rate equations for semiconductor lasers subjected to simultaneous near-resonant optical injection and microwave current modulation are examined by combined analytical-numerical bifurcation techniques. Simple qualitative criteria are given for a bistable response. These results compare well with experimental measurements.

DOI: 10.1103/PhysRevE.65.056610 PACS number(s): 42.65.Sf, 42.60.Fc, 42.65.Pc, 42.55.Px

I. INTRODUCTION

Bistability of pulsating regimes for weakly periodically forced oscillators is a well known phenomenon for mechanical or electronic systems such as the driven Duffing or van der Pol oscillators [1,2]. It is, however, poorly documented for lasers exhibiting limit-cycle intensity oscillations such as semiconductor lasers subject to optical injection. Cases of bistability have been reported for periodically modulated semiconductor lasers but under strong modulation conditions and between different periodic states such as period-1 and period-2 regimes [3–6]. Bistability under weak modulation conditions is less well known for lasers in general [7] but this problem was revived by recent experiments using optically injected diode lasers at high injection rates [8]. In these experiments, cw optical injection induces a limit-cycle instability in the optical output. When a small periodic current modulation is added to the dc bias current remarkable limit-cycle phase locking performances have been obtained. The laser is doubly locked to the cw optical injection and the microwave current modulation. The output power exhibits a deep, high quality microwave oscillation. A similar performance has been observed previously by using sideband injection locking where a semiconductor laser is stably locked to a modulation sideband of a master laser [9–13]. Such devices are promising for a number of applications that require a spectrally pure microwave oscillator with frequencies in the tens of gigahertz. A bistable output means that two distinct amplitudes of the oscillations are available for certain values of the control parameters. As we shall demonstrate analytically and show with experimental measurements, bistability can be achieved under strong optical injection with simultaneous weak current modulation, although the domain of parameters is not obvious.

In this paper, we model such a double-locking experiment using the laser rate equations, which are then analyzed by combined analytical and numerical bifurcation techniques. Our objective is to determine simple conditions for bistability which will guide our experiments. In our previous analysis of the laser equations [14,15], the optical detuning was assumed zero, and we analyzed the laser response as a function of the optical injection rate. We found several branches of periodic and quasiperiodic intensity oscillations but no case of bistability. Our present analysis of the laser equations takes the optical detuning instead of the injection rate as the control parameter and leads to cases of bistability.

The paper is organized as follows. In Sec. II, we formulate the laser rate equations and derive a slow time amplitude equation. The solutions of this equation are then analyzed analytically and numerically and the possible bifurcation diagrams are shown in Sec. III. We emphasize the domains of bistability in the injection rate versus detuning diagrams. Section IV is devoted to the experiments and the main results are summarized in Sec. V.

II. FORMULATION AND AMPLITUDE EQUATION

Most of our understanding of the effects of optical injection in a single-mode diode laser comes from numerical and analytical studies of simple rate equations for the complex electric field $\mathcal{E}$ and the excess carrier number Z. The formulation of dimensionless rate equations is documented in several places. Introducing the current modulation, these equations are given by [15]

$$\frac{d\mathcal{E}}{dt}=(1+i\alpha)Z\mathcal{E}+i\Omega\mathcal{E}+\Lambda, \tag{1}$$

$$T\frac{dZ}{dt}=P[1+\delta\cos(\omega t)]-Z-(1+2Z)|\mathcal{E}|^2. \tag{2}$$

Here time t is measured in units of the photon lifetime. Λ denotes the amplitude of the injected signal. δ and ω describe the modulation depth and the frequency of the current modulation, respectively. P is the average value of the dimensionless pumping current above threshold. The fixed parameters α and T are the linewidth enhancement factor, which measures the degree of amplitude-phase coupling, and the ratio of carrier lifetime to photon lifetime, respectively. T is typically an $O(10^3)$ large quantity which allows important

simplifications in our analysis. Finally, Ω is defined as the detuning between slave and master optical frequencies.

In the absence of modulation, the steady output solutions and their stability boundaries are available analytically [16]. For a range of detuning values, there exists a threshold value Λ_H of the optical injection rate above which the intensity limit-cycle oscillations vanish in favor of a steady output. Such a threshold is known as a Hopf bifurcation. Moreover, conditions of resonance between the modulation frequency ω and the limit-cycle frequency ω_H at the Hopf bifurcation ($\omega_H = \omega$) can be determined analytically (see Appendix A in [15]). For fixed values of the laser parameters α, Ω, T, and P, these conditions lead to critical values for Λ and ω which we denote by $\Lambda = \Lambda^*$ and $\omega = \omega^*$. Our analysis assumes that (i) the laser operates close to the Hopf bifurcation point ($\Lambda \simeq \Lambda^*$), (ii) the detuning $|\Omega|$ and the modulation amplitude δ are small, and (iii) the modulation frequency is nearly resonant ($\omega \simeq \omega^*$), which is a necessary condition for phase locking. A two-time perturbation analysis [17] allows us to construct a periodic solution in the vicinity of this point. The leading approximation of the intensity is given by

$$|\mathcal{E}|^2 = |\mathcal{E}_0|^2 + R\cos(\omega t + \phi) + O(R^2) \tag{3}$$

where $|\mathcal{E}_0|^2$ is the steady state intensity at the Hopf bifurcation point. The small amplitude oscillations are sinusoidal in first approximation with amplitude R and phase ϕ. They both change slowly with respect to time and the complex amplitude $A = R\exp(i\phi)$ satisfies an equation of the form

$$ik_\omega \frac{dA}{dt} = k_\delta \delta + A[k_\omega(\omega - \omega^*) + k_\Lambda(\Lambda - \Lambda^*) + k_\Omega \Omega - k_3|A|^2]. \tag{4}$$

The derivation of such an equation is well documented for simple oscillator problems [1,2]. For problems like our laser equations (1) and (2), the perturbation analysis is algebraically longer but the asymptotic method is technically the same. This is an extension of our previous analysis [15]: for $\Omega = 0$, Eq. (4) is equivalent to Eq. (16) in [15]. The complex coefficients appearing in Eq. (4) are of the form $k_\omega = c_\omega/\omega^*$, $k_\delta = c_\delta$, $k_\Lambda = c_\Lambda/\Lambda^*$, and $k_\Omega = c_\Omega/\omega^*$ where the c_j have been simplified by taking the limit T large and checked using the symbolic computation software MAPLE. They depend only on the linewidth enhancement factor α.

III. BIFURCATION DIAGRAMS

Steady state solutions of Eq. (4) mean phase-locked limit cycles of the laser equations, whereas periodic solutions mean intensity pulsations with a slowly varying phase. These solutions are obtained numerically by using the continuation software AUTO [18]. The application of continuation methods for amplitude equations like (4) is rare but allows a determination of both stable and unstable branches of periodic solutions, and, therefore, a better understanding of the laser bifurcation possibilities. Figures 1(a)–1(e) represent six different bifurcation diagrams. Each figure illustrates a typical double-locking experiment for progressively larger values of the modulation strength δ. During each measurement, a control parameter (chosen here as the optical detuning Ω) is quasistatically swept across the phase-locking range. The other parameters have been fixed to $\Lambda = \Lambda^*$, $\omega - \omega^* = \omega_1 > 0$, and $\alpha = 5$. Compared to our previous study of the perfectly tuned laser [15], we now note the possibility of bistable responses. Bistability means that two stable solutions may coexist for a range of values of the sweeping parameter Ω [see Figs. 1(c), 1(d), and 1(e)]. Note that a bistable output does not exist for arbitrarily small values of the modulation strength δ. Moreover, two kinds of bistability may be distinguished. First, from Figs. 1(d) and 1(e), we observe the coexistence of two distinct branches of phase-locked solutions. Second, Fig. 1(c) also shows a small region of bistability between a locked state and a quasiperiodic state.

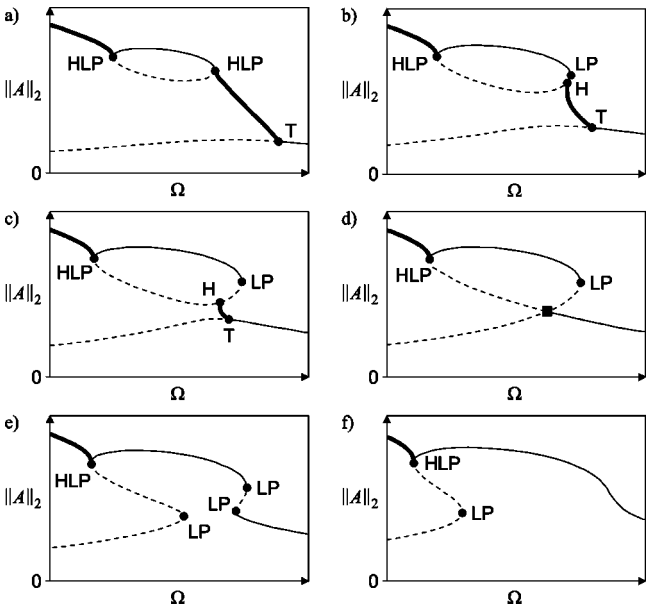

FIG. 1. One-parameter bifurcation diagrams.The figure represents the root-mean-square average $\|A\|_2$ of the amplitude of the oscillations (measured in arbitrary units) as a function of the optical detuning Ω (measured in arbitrary units and with an arbitrary offset). Frames (a) to (f) correspond to increasingly high values of the modulation strength δ. All other parameters are fixed. In particular, $\alpha = 5$. The thin solid and dashed lines represent the stable and unstable steady solutions of Eq. (4), respectively. According to Eq. (3), these solutions correspond to phase-locked, periodic intensity pulsations of the original laser equations (1) and (2). Unstable solutions are unobservable experimentally. The thicker lines represent periodic solutions of Eq. (4). They are all stable and, using Eq. (3), these solutions correspond to branches of oscillating solutions of the original laser equations (1) and (2) with a slowly varying phase. The critical bifurcation points are marked in the figures. LP means limit point or saddle-node bifurcation point; T means a torus bifurcation point from phase-locked (periodic) to variable phase (quasiperiodic) oscillations; H and HLP refer to a homoclinic (or infinite period) periodic solution and a homoclinic limit point, respectively.

An alternative description of the dynamics is shown in Fig. 2. In this figure, we represent the regions of qualitatively different regimes in the δ versus Ω parameter space. Both kinds of bistability domain correspond to the two roughly

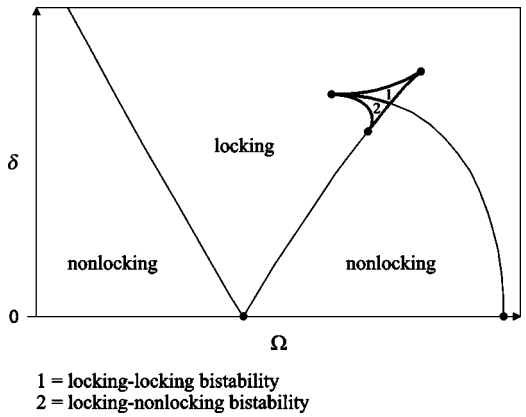

FIG. 2. Two-parameter map of the dynamics for $\alpha=5$. The different dynamical regimes predicted by Eq. (4) are shown in the δ (arbitrary units) versus Ω (arbitrary units and offset) diagram. Note the existence of two distinct bistability regimes.

triangular shapes in the upper right corner of the figure. We contrast this diagram with the dynamics map in the δ versus Λ parameter space discussed in [15], and reproduced here as Fig. 3. We noted no domain of bistability for realistic values of δ, which suggests that only experiments with the detuning as the sweeping parameter may lead to the observation of bistability. This point is further discussed in Sec. V. A successful observation of bistability requires that its domain in parameter space is large enough. We have found that it tends to expand for larger values of linewidth enhancement factor α.

IV. EXPERIMENTS

The theory predicts that a bistable output is possible if we sweep back and forth the optical detuning instead of the injection rate and if the modulation amplitude surpasses a threshold. The experimental configuration used to study the bistability characteristics has been described previously [8]. Both master and slave lasers, high speed variants of SDL model 5400 series lasers, are under separate temperature and current control. The master laser output is passed through a variable attenuator, optical isolator, and beam splitter before

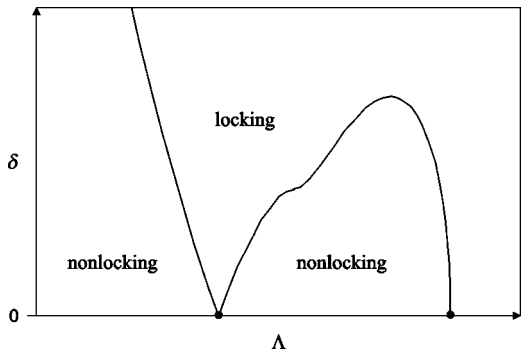

FIG. 3. Two-parameter map of the dynamics for $\alpha=5$. The different dynamical regimes predicted by Eq. (4) are shown in the δ (arbitrary units) versus Λ (arbitrary units and offset) diagram. Note that there is no observable domain of bistability.

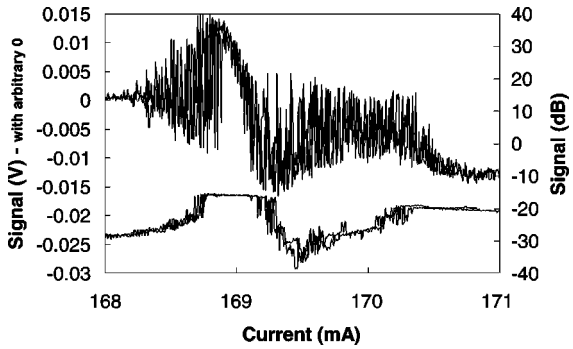

FIG. 4. Output voltage from the microwave mixer (top curves and left axis) and power at the modulation frequency (bottom curves and right axis) under weak current modulation.

injection into the slave. Temperature and current control is used to bring the optical frequencies of the two lasers into near resonance. The attenuator adjusts the amplitude of the optical injection. The slave laser is operated at a bias of approximately five times the threshold value, and a microwave modulation current from a frequency synthesizer is added to the bias. After being split off at the beam splitter, the output from the slave laser is passed through additional optical isolators and detected by a fast photodiode. The photodiode signal is amplified and split with one arm going to a microwave spectrum analyzer and the other to a microwave mixer. At the mixer the signal is compared with the signal from the microwave frequency synthesizer and a digitizing oscilloscope detects the resulting intermediate frequency signal. The output voltage from the mixer tracks the phase offset when the two input signals are frequency locked while it varies rapidly when they are not. Tuned to the frequency of the synthesizer, the microwave spectrum analyzer is used to measure the power at the reference frequency.

The master and slave lasers are biased so that optical injection causes the slave laser to operate near the Hopf bifurcation. The injected optical power is on the order of 0.01 of the free-running output from the slave laser, and the master laser is slightly detuned to an offset of a few gigahertz below the free-running optical frequency of the slave. In the results presented here, the dc bias to the master laser is slowly varied. While this produces a small change in the amplitude of the injection signal, the primary effect is to vary the optical frequency of the master laser at a rate of approximately -2.8 GHz/mA. Varying the optical frequency of the master laser causes the dc-biased slave laser to move from stable, locked operation to limit-cycle dynamics and the frequency of the resonance to vary. An added modulation current to the slave laser that is fixed in frequency and amplitude allows us to view the changes in dynamics as the bias to the master laser is varied.

Figures 4 and 5 show measurements at two different powers of the modulation signal that illustrate the changes in the dynamics near the Hopf point. The modulation frequency was fixed at 7.63 GHz. For weak modulation currents, Fig. 4, two locking domains are observed. First, a region of periodic oscillations corresponding to the small amplitude modulation of the stable steady state above the Hopf point appears for

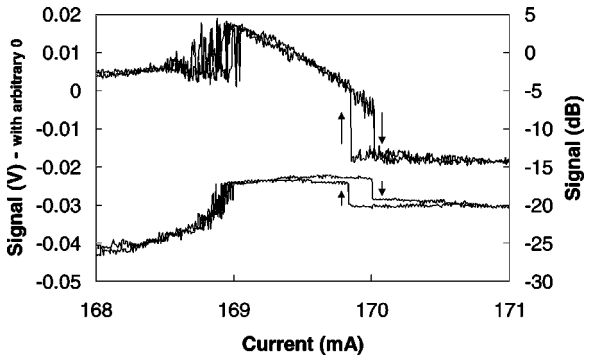

FIG. 5. Output voltage from the microwave mixer (top curves and left axis) and power at the modulation frequency (bottom curves and right axis). The current modulation is 7 dB greater in power than for the data in Fig. 4.

master laser currents above approximately 170.3 mA. Second, a region of resonantly locked oscillations corresponding to the small amplitude modulation of the limit-cycle oscillations below the Hopf point was centered about 169 mA. Both these regions show relatively weak fluctuations in the power at the modulation frequency and the latter also shows a relatively strong locked power. Outside these two regions, quasiperiodic oscillations are observed as indicated by the strong fluctuations of the mixer signal and the optical power. The experiment clearly illustrates the bifurcation diagram of Fig. 1(a). When the modulation power is increased by 7 dB the stronger modulation currents cause the two regions to merge, as shown in Fig. 5. The smoothly varying mixer voltage, and a relatively strong locked power, indicate the region of locked periodic dynamics between approximately 169 and 170 mA. Note the region of bistability at the edge of this locked region as the laser makes the transition to limit-cycle dynamics due to modulation of the stably locked laser. The arrows give the direction of the sweep and the transition. The experiment illustrates the bifurcation diagrams of Figs. 1(d) and 1(e). No bistability is observed for modulation powers 2 dB below those used for the data in Fig. 5, which agrees with the condition of a sufficiently high modulation amplitude.

V. DISCUSSION

A laser exhibiting limit-cycle oscillations may either lock to a weakly modulated signal or sustain quasiperiodic oscillations with two frequencies, namely, the frequency of the modulations and the difference between modulation and solitary laser frequencies. This is the typical response of a limit-cycle oscillator driven by a small amplitude and near-resonant modulation. The effect of the nonlinearity is to bend the amplitude curve, allowing multivalued regions. If a low and a high amplitude solution may coexist and are stable, we have a case of bistability that we may observe by sweeping back and forth the control parameter. Transitions between low and high amplitude regimes then occur through jumps that can be identified experimentally. By using Hopf bifurcation techniques and determining bifurcation diagrams, we have found conditions of bistability in terms of the optical detuning. However, the domain of bistability is relatively small and requires that the modulation amplitude is sufficiently large and that the linewidth enhancement factor is not too low so that the effects of nonlinearity are maximized. These conditions guided our experiments shown in Fig. 5, clearly showing the jumps between high and low states.

To understand why bistability is not possible if we consider the optical injection as the control parameter [15], we need to realize that we modulate a limit-cycle oscillator generated by a Hopf bifurcation rather than a conservative oscillator like the Duffing mechanical oscillator. As seen in Fig. 1, locking occurs at a specific limit-cycle amplitude at zero modulations and, as we progressively increase the driving amplitude, this point grows into an isolated branch of locked solutions. This isola naturally coexists with a small amplitude periodic solution. Provided the size of the isola is sufficiently large, coexistence of two stable regimes is possible as we may see in Figs. 1(c)-1(e). This phenomenon occurs if we use the detuning as the control parameter but not if we consider the injection rate (see Figs. 1-5 in [15]). There, the isola never reaches a size that allows its overlap with a small amplitude stable regime, for realistic values of the laser parameters.

ACKNOWLEDGMENTS

The research of A.G. and V.K. was supported by the U.S. Air Force Office of Scientific Research. The research of T.E. was supported by the U.S. Air Force Office of Scientific Research through Grant No. AFOSR F49620-98-1-0400, the National Science Foundation through Grant No. DMS-9973203, the Fonds National de la Recherche Scientifique (Belgium), and the InterUniversity Attraction Pole of the Belgian government. The research of M.N. was supported by the Fonds National de la Recherche Scientifique (Belgium). The research of T.B.S. was supported in part by the U.S. Army Research Office under Contract No. DAAG-55-98-C-0038, and by the U.S. Air Force Research Laboratory under Contract No. F29601-00-C-0001.

[1] P. G. Drazin, *Nonlinear Systems*, Cambridge Texts in Applied Mathematics (Cambridge University Press, Cambridge, England, 1992).

[2] A. H. Nayfeh and D.T. Mook, *Nonlinear Oscillations* (Wiley-Interscience, New York, 1979).

[3] H. Kawaguchi, *Bistabilities and Nonlinearities in Laser Diodes* (Artech House, Boston, 1994).

[4] Chang-Hee Lee, T.-H. Yoon, and S.-Y. Shin, Appl. Phys. Lett. **46**, 95 (1985).

[5] Y.C. Chen, H.G. Winful, and J.M. Liu, Appl. Phys. Lett. **47**, 208 (1985).

[6] G.P. Agrawal, Appl. Phys. Lett. **49**, 1013 (1986).

[7] J.C. Celet, D. Dangoisse, P. Glorieux, G. Lythe, and T. Erneux, Phys. Rev. Lett. **81**, 975 (1998).

[8] T.B. Simpson, Opt. Commun. **170**, 93 (1999); T.B. Simpson and F. Doft, IEEE Photonics Technol. Lett. **11**, 1476 (1999).
[9] L. Goldberg, H.F. Taylor, and J.F. Weller, Electron. Lett. **18**, 1019 (1982).
[10] L. Noel, D. Wake, D.G. Moodie, D.D. Marcenac, L.D. Westbrook, and D. Nesset, IEEE Trans. Microwave Theory Tech. **45**, 1416 (1997).
[11] C. Walton, A.C. Bordonalli, and A. Seeds, IEEE Photonics Technol. Lett. **10**, 427 (1998).
[12] R.-P. Braun, G. Grosskopf, D. Rohde, and F. Schmidt, IEEE Photonics Technol. Lett. **10**, 728 (1998).
[13] C. Laperle, M. Svilans, M. Poirier, and M. Tetu, IEEE Trans. Microwave Theory Tech. **47**, 1219 (1999).
[14] A. Gavrielides, V. Kovanis, T. Erneux, and M. Nizette, Proc. SPIE **3944**, 627 (2000).
[15] M. Nizette, T. Erneux, A. Gavrielides, and V. Kovanis, Phys. Rev. E **63**, 026212 (2001).
[16] A. Gavrielides, V. Kovanis, and T. Erneux, Opt. Commun. **136**, 253 (1997).
[17] J. Kevorkian and J. D. Cole, *Multiple Scale and Singular Perturbation Methods*, Applied Mathematical Sciences Vol. 114 (Springer, New York, 1996).
[18] E. Doedel, T. Fairgrieve, B. Sandstede, A. Champneys, Yu. Kuznetsov, and X. Wang, http://indy.cs.concordia.ca/auto/main.html.